IUST
Iran University of Science and Technology

Iranian Journal of Electrical and Electronic Engineering

Journal Homepage: ijeee.iust.ac.ir

Multivariable Prediction Control for Direct Vector Control of a DFIG-based Wind Turbine using a Fuzzy Space Vector Modulation Converter

Azzedine khati*(C.A.)

Abstract: In this research paper, a multivariable prediction control method based on direct vector control is applied to command the active power and reactive power of a doubly-fed induction generator used into a wind turbine system. To obtain high energy performance, the space vector modulation inverter based on fuzzy logic technique (fuzzy space vector modulation) is used to reduce stator currents harmonics and active power and reactive power ripples. Also the direct vector control model of the doubly-fed induction generator is required to ensure a decoupled control. Then its classic proportional integral regulators are replaced by the multivariable prediction controller in order to adjust the active and reactive power. So, in this work, we implement a new method of control for the doubly-fed induction generator energy. This method is carried out for the first time by combining the MPC strategy with artificial intelligence represented by Fuzzy SVM-based converter in order to overcome the drawbacks of other controllers used in renewable energies. The given simulation results using Matlab software show a good performance of the used strategy, particularly with regard to the quality of the energy supplied.

Keywords: Doubly-fed induction generator (DFIG), fuzzy logic, multivariable prediction control (MPC), space vector modulation (SVM), direct vector control (DVC), artificial intelligent (AI).

1 Introduction

DESPITE the DFIG has the drawback of the presence of collector-brushes which makes it less robust and requires regular maintenance, its use continues to increase in renewable energies taking into account its operating principle which allows to adjust the power on the rotor in order to manage the power provided to grid thanks to the connection between the rotor and the grid [1-2]. This broad interest is evident in the large number of research and publications that treat the use of DFIG in Wind Turbine System (WTS) [3-4]. On the other hand, several kinds of control were used for the speed, torque and power control of DFIG such as Neural Network Control (NNC) [5], Sliding Mode Control (SMC) [6-7], Field Oriented Control (FOC) [8], Backstepping Control (BC) [9-10]...etc. However, these methods give high Total Harmonic Distortion (THD) of currents of stator and important power ripples [2-11], especially when they employed with Pulse Width Modulation (PWM) inverters. These latter are often used in electrical machines control. Nevertheless, they also give more harmonics in terms of flux, power and torque. To compensate for this disadvantage, [12] proposed a new method to control the converter. It's SVM. Its advantage is that it gives a minimal THD where the principle is detailed in [13]. On the other hand, this method also has drawbacks including variable switching frequency and high ripples due to hysteresis regulators.

To improve the performances of active and reactive powers control of DFIG, in this article, we propose a new control strategy. That of replacing the hysteresis controllers and DVC with fuzzy logic controllers based MPC.

The idea of choosing a MPC is to compensate for multiple controllers when there are more variables to

Iranian Journal of Electrical & Electronic Engineering, 2024.
Paper first received 20 January 2024 and accepted 16 September 2024.
* The author is with the Department of Mechanical Engineering, Hassiba Benbouali University, Chlef, Algeria.
E-mail: a.khati@univ-chlef.dz.
Corresponding Author: Azzedine Khati.

control, with a single controller in order to reduce calculations and minimize the control system size. On the other hand, the predictive control is simple to design and implement compared to the conventional control method and highly developed in terms of dynamic response, execution time and flexibility [14]. It has also proven its effectiveness in industrial applications [15]. In addition, the AI is also used in this article, represented by fuzzy SVM controllers, to generate the control pulses of inverter. The fuzzy logic rules are written by absorbing the performances of the hysteresis controller and the variable to be adjusted.

This article is organized according to the following strategy: we presented the DFIG in the d-q reference model. Then the DVC of DFIG with inverter fuzzy SVM are detailed. And we have given a brief description of MPC before synthetizing the scheme of the control of the DFIG active and reactive power. This work is closed with a conclusion and perspectives for future work.

2 DFIG Park model

The DFIG is given in the Park (d-q) model by the following equations [2]:

$$\begin{cases} V_{sd} = R_s.I_{sd} + \frac{d\psi_{sd}}{dt} - \omega_s.\psi_{sq} \\ V_{sq} = R_s.I_{sq} + \frac{d\psi_{sq}}{dt} + \omega_s.\psi_{sd} \\ \omega_r = \omega_s - p.\Omega \\ V_{rd} = R_r.I_{rd} + \frac{d\psi_{rd}}{dt} - \omega_r.\psi_{rq} \\ V_{rq} = R_r.I_{rq} + \frac{d\psi_{rq}}{dt} + \omega_r.\psi_{rd} \end{cases} \quad (1)$$

$$\begin{cases} \psi_{sd} = L_s.I_{sd} + M.I_{rd} \\ \psi_{sq} = L_s.I_{sq} + M.I_{rq} \\ \psi_{rd} = L_r.I_{rd} + M.I_{sd} \\ \psi_{rq} = L_r.I_{rq} + M.I_{sq} \end{cases} \quad (2)$$

Where,

R_s, R_r, L_s, L_r and M : Rotor and stator parameters of the generator.
V_{sd}, V_{sq}, V_{rd} and V_{rq} : Stator and rotor voltages.
I_{sd}, I_{sq}, I_{rd} and I_{rq} : Stator and rotor currents.
ψ_{sdq} and ψ_{rdq} : Stator and rotor flux.
ω_s and ω_r : Stator and rotor pulsation.
Ω: Mechanical speed.
p: Number of pair of poles

The mechanical equation of the system is given by:

$$T_e = T_r + J\frac{d\Omega}{dt} + f\Omega \quad (3)$$

Where:
T_e: Electromagnetic torque
T_r: Load torque
J: Inertia
f: Viscous friction coefficient

Moreover, the electromagnetic torque can be written as:

$$T_e = p.M(I_{rd}.I_{sq} - I_{rq}.I_{sd}) \quad (4)$$

As well as the active power and the reactive power of the stator are expressed as follows:

$$\begin{cases} P_s = \frac{3}{2}(V_{sd}.I_{sd} + V_{sq}.I_{sq}) \\ Q_s = \frac{3}{2}(V_{sq}.I_{sd} - V_{sd}.I_{sq}) \end{cases} \quad (5)$$

Where:
P_s: Stator's active power, Q_s: Stator's reactive power

3 DVC command strategy

The principle of this command is to align the stator flux vector on the "d" axis in order to eliminate it along the "q" axis [5] (fig. 1).

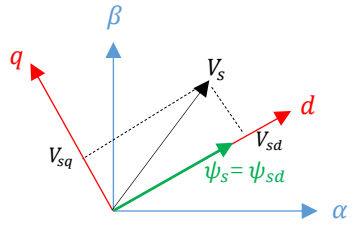

Fig. 1 stator flux oriented along the "d" axis

$\psi_s = \psi_{sd}$ and $\psi_{sq} = 0$

With negligible R_s from (1), we can write:

$$\begin{cases} V_{sd} = 0 \\ V_{sq} = \omega_s.\psi_{sd} \end{cases} \quad (6)$$

$$\begin{cases} I_{sd} = -\frac{M}{L_s}I_{rd} + \frac{\psi_s}{L_s} \\ I_{sq} = -\frac{M}{L_s}I_{rq} \end{cases} \quad (7)$$

And (5) becomes:

$$\begin{cases} P_s = -\frac{3}{2}\frac{\omega_s\psi_s M}{L_s}I_{rq} \\ Q_s = -\frac{3}{2}\left(\frac{\omega_s\psi_s M}{L_s}I_{rd} - \frac{\omega_s\psi_s^2}{L_s}\right) \end{cases} \quad (8)$$

Also (4) becomes:

$$T_e = -\frac{3}{2}p.\frac{M}{L_s}.I_{rq}.\psi_s \quad (9)$$

The fig. 2 shows the principle of DVC technique with SVM inverter for controlling the DFIG. On the other hand, the DVC structure without current loop is shown in fig. 3.

This method is also known as Field-Oriented Control (FOC).

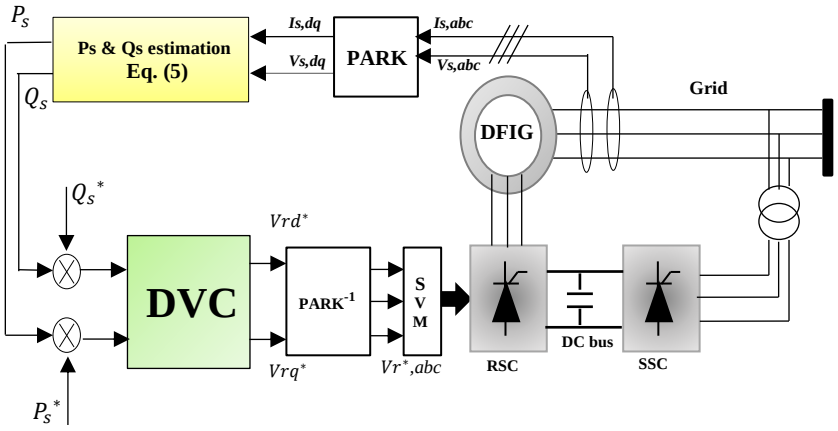

Fig. 2 DVC of DFIG scheme

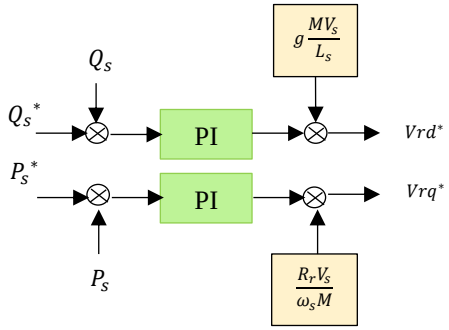

Fig. 3 DVC structure without current loop

4 Fuzzy SVM

The inverter can be controlled by several methods. Many research used PWM. Others use other methods as Discrete Pulse Width Modulation (DPWM) which is applied in [16]. Also [17] proposed SVM technic. This latter is too employed to modulate the inverters. Its principle is based on the calculation of angles and parameters of sectors. But [11] propose a new SVM inverter without calculating sectors and angles. The principle of which is to compute the maximum and the minimum of balanced voltages (Fig. 4). This SVM has some advantages because it needs no sector identifications, angle information is not needed and no lookup table is used to calculate switching times. Moreover, it has high performance in real-time control systems [18].

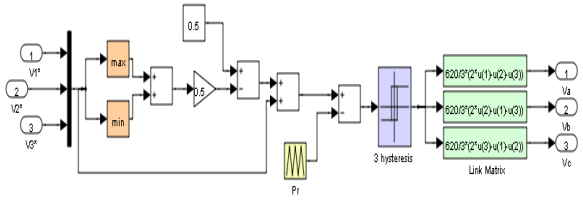

Fig. 4 SVM inverter command

In this section, we propose to replace the hysteresis blocks in SVM with fuzzy logic controllers to enhance performances of the control. This strategy is called Fuzzy SVM (Fig. 5). On other hand, Fuzzy logic technology does not have a complex mathematical model [19]. Furthermore, the Fuzzy SVM gives minimum harmonic distortion of stator currents.

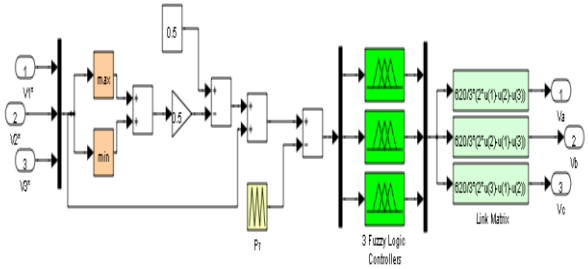

Fig. 5 Fuzzy SVM inverter

Fig. 6 shows the Fuzzy logic main structure. The proposed Fuzzy Logic controller is based on hysteresis controllers. The most popular fuzzy controller is the e-Δe controller. It is a two-input fuzzy controller and a command output.

e = error; Δe = error variation

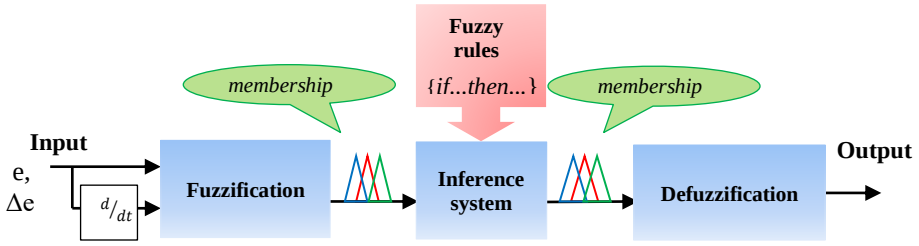

Fig. 6 Internal Structure of Fuzzy Rules

For the synthesis of a fuzzy command, it is necessary to choose the linguistic information model, the inference process, the aggregation process and also the defuzzification process.

Fuzzy controller design is based on intuition and simulation experience. Often, the number of sets is based on domain knowledge. In this work, we have realized for the input variables and the output variable a 7 set fuzzy controller, with the aim of finding the desired good performances for the adjustment taking into account the balance between precision and computational cost. This is a reasonable choice, as it allows for a good balance between granularity and complexity. Also, 7 sets is often considered a good choice because it allows for fine granularity while remaining manageable. And are generally easy to understand and work with. In addition, 7 linguistic terms are commonly used in fuzzy logic literature and applications. With 2 inputs and 7 sets each, we'll have 49 possible rules. This is complex enough to capture many scenarios without becoming unmanageable.

The linguistic values are defined for the linguistic variables *e* and *Δe* as follows:

Negative Big **(N.B)**, Negative Middle **(N.M)**, Negative Small **(N.S)**, Positive Small **(P.S)**, Positive Big **(P.B)**, Positive Middle **(P.M)**, Equal Zero **(E.Z)**.

The membership function definition for the input and output is given by Fig. 7:

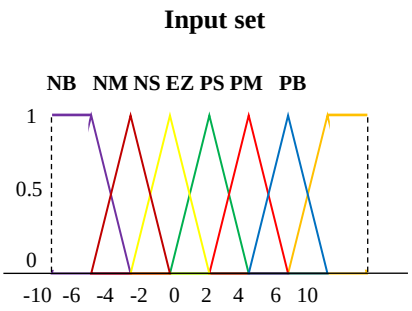

Fig. 7.a Membership function for the inputs

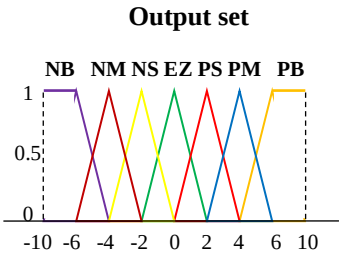

Fig. 7.b Membership function for the output

The fuzzy rules governing this system thus take the following form:

$\{IF\ e\ is\ N.B\ and\ \Delta e\ is\ N.B\ THEN\ s\ is\ N.B$

$(IF\ e\ is\ N.B\ and\ \Delta e\ is\ N.M\ THEN\ s\ is\ N.B$

$\vdots$

$\{IF\ e\ is\ P.B\ and\ \Delta e\ is\ P.M\ THEN\ s\ is\ P.B$

The rules were formulated using analysis data obtained from the simulation of the system using different values of rotor voltages. The 7 fuzzy sets, defined by their membership functions, for each of e and Δe respectively, make it possible to construct 49 rules. These rules are given in table 1[20].

Table 1 Inference matrix

e / Δ.e	N.B	N.M	N.S	E.Z	P.S	P.M	P.B
N.B	N.B	N.B	N.B	N.B	N.M	N.S	E.Z
N.M	N.B	N.B	N.B	N.M	N.S	E.Z	P.S
N.S	N.B	N.B	N.M	N.S	E.Z	P.S	P.M
E.Z	N.B	N.M	N.S	E.Z	P.S	P.M	P.B
P.S	N.M	N.S	E.Z	P.S	P.M	P.B	P.B
P.M	N.S	E.Z	P.S	P.M	P.B	P.B	P.B
P.B	E.Z	P.S	P.M	P.B	P.B	P.B	P.B

Fig.8 shows Fuzzy controller parameters, (Just type ">> fuzzy" in the MATLAB workspace window, and the following figure appears).

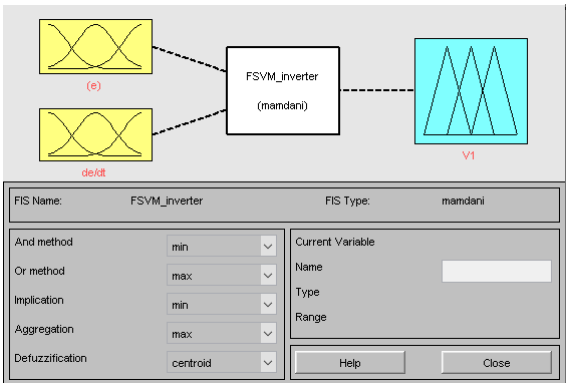

Fig. 8 Fuzzy controller parameters

The synthesized fuzzy SVM will be used to control the rotor side inverter of the DFIG with the control strategy cited below (Fig. 9).

5 Multivariable Predictive Control

The Predictive Control technique relies on the dynamic model of the system in real time to anticipate the future behavior of the system. It's used to control complex systems [14]. On the other hand, its applications in digital control domains have given good results in terms of response time and precision [21]. The description of the method is detailed in [15]. In this work, we use the MIMO (multi-inputs/multi-outputs) prediction strategy in accordance with our process model of which it has two inputs and two outputs to control the DFIG. The two PI regulators of active and reactive powers and the rotor currents in the DVC will be replaced by a MPC (fig. 9).

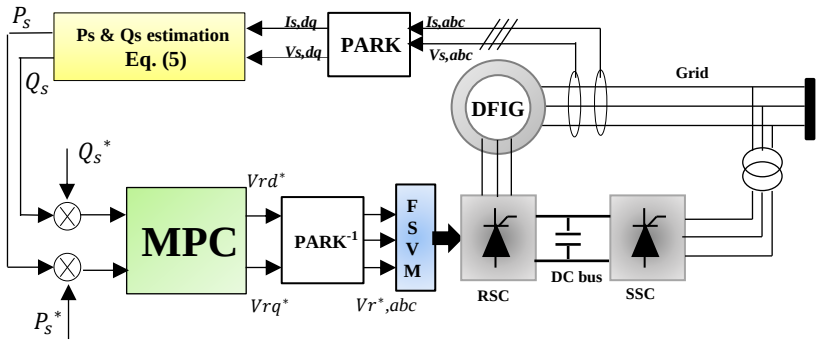

Fig. 9 MPC based on fuzzy SVM for the DFIG

Active and reactive power are given by state estimation according to eq (5).

5.1 Determination of System Matrix

The multivariable system in Z-transformation is given by [22].

$$\begin{cases} z^{-1}.X(z^{-1}) - x_0 = A.X(z^{-1}) + B.U(z^{-1}) \\ Y(z^{-1}) = C.X(z^{-1}) + D.U(z^{-1}) \end{cases} \quad (10)$$

Where:
$X(z) = Z[\mathrm{x(k)}]$, $U(z) = Z[u(k)]$ and $Y(z) = Z[y(k)]$

The transfer matrix linking the inputs to the outputs is given by:

$$Y(z^{-1}) = [C(z.I - A)^{-1}.B + D].U(z^{-1}) \quad (11)$$
$$Y(z^{-1}) = G(z^{-1}).U(z^{-1}) \quad (12)$$
$$G(z^{-1}) = [C(z^{-1}.I - A)^{-1}.B + D] \quad (13)$$

Where: $G(z^{-1}) \in C^{n\times m}$
With: *n*: Input number and *m*: Output number.

The process model can take different representations (by transfer function, by state space, impulse response, etc.). For our formulation, the system is represented in the CARIMA form (Controlled Auto-Regressive Integrated Moving Average) whose expression is [13] [23]:

$$A(z^{-1})y(k) = z^{-1}B(z^{-1})u(k) + \frac{C(z^{-1})\xi(k)}{\Delta(z^{-1})} \quad (14)$$

With:
$A(z^{-1})$: input matrix, $B(z^{-1})$: output matrix,
$\xi(k)$: white noise centered, z^{-1}:the delay operator, $\Delta(z^{-1}) = 1 - z^{-1}$: integral action in the corrector , $C(z^{-1})$: disturbance matrix and $u(k)$ *:* control matrix.
Where:

$$\begin{cases} A(z^{-1}) = 1 + a_1 z^{-1} + \ldots\ldots a_{na} z^{-na} \\ B(z^{-1}) = b_0 + b_1 z^{-1} + \ldots\ldots b_{nb} z^{-nb} \\ C(z^{-1}) = 1 + c_1 z^{-1} + \ldots\ldots c_{nc} z^{-nc} \end{cases} \quad (15)$$

However, the determination of matrix $A(z^{-1})$ and $B(z^{-1})$ is not like the case of a monovariable system, whose the polynominal are determined from the transfer matrix $G(z^{-1})$.On the other hand, in the multivariable system, to determinate $A(z^{-1})$ and $B(z^{-1})$ we have:

$$G(z^{-1}) = A(z^{-1})^{-1}B(z^{-1})z^{-1} \quad (16)$$

The simplest is to take $A(z^{-1})$ as a diagonal matrix, and their diagonal elements are the smallest common multiples of the denominators of the corresponding lines of $G(z)$ [15]. Therefore, $B(z^{-1})$ is computed by:

$$B(z^{-1}) = A(z^{-1})\, G(z^{-1})\, z \tag{17}$$

5.2 J-step MIMO system system predictions

The prediction equation of MIMO system is given [24]:

$$\hat{y}(k+1) = H_j(z^{-1})\Delta u(k+j-d) + E(k+j) \tag{18}$$

Where:

$$E(k+j) = \frac{G_j(z^{-1})y(k)+J_j(z^{-1})\Delta u(k-1)}{A_m(z^{-1})C(z^{-1})} \text{ free response} \tag{19}$$

$$H_j(z^{-1})\Delta u(k+j-d) \quad \text{forced response} \tag{20}$$

With: $H_j(z^{-1}), J_j(z^{-1}) : matrix^{n\times m}$

$E(k+1)$: $vector^{n\times 1}$

$$\begin{cases} \hat{y}(k+1) = H_1(z^{-1})\Delta u(k+1-d) + E(k+1) \\ \hat{y}(k+1) = H_2(z^{-1})\Delta u(k+1-d) + E(k+2) \\ \hat{y}(k+1) = H_3(z^{-1})\Delta u(k+1-d) + E(k+3) \\ \quad \vdots \\ \hat{y}(k+1) = H_{N_2}(z^{-1})\Delta u(k+1-d) + E(k+N_2) \end{cases} \tag{21}$$

The matrix expression of (18) is:

$$Y = H.U + E \tag{22}$$

5.3 The optimal predictor

As in the case of a monovariable, in order to calculate an optimal sequence of the command signal, we apply a quadratic cost function to the prediction values of (23) [14-15]:

$$J_{GPC} = \sum_{j=N_1}^{N_2} \left[\hat{y}(k+j) - w_{ref}(k+j)\right]^2 + \lambda \sum_{j=1}^{N_u} [\Delta u(k+j-d)]^2 \tag{23}$$

Where:

N_1 : Minimum prediction horizon, N_2 :Maximum prediction horizon, N_u : Command horizon and λ :Weighting factor.

By substituting (22) into (23), multidimensional cost function is given:

$$J = (HU + E - W)^T(HU + E - W) + \lambda U^T U \tag{24}$$

To minimize (24), it is first developed in distinct terms [25]:

$$J_{GPC} = U^T(H^T H + \lambda I)U + U^T H^T(E-W) + (E-W)^T HU + (E-W)^T(E-W) \tag{25}$$

Because:

$$U^T H^T(E-W) = (E-W)^T HU \tag{26}$$

J can be simplified:

$$J_{GPC} = U^T(H^T H + \lambda I)U + 2U^T H^T(E-W) + (E-W)^T(E-W) \tag{27}$$

Finally, the optimal sequence of future commands is obtained by analytical minimization of the criterion in matrix form $\frac{dJ}{d\vec{U}} = 0$ [26]:

$$\vec{U} = \left(H^T H + \lambda I_{N_u}\right)^{-1} H^T(W - E) \tag{28}$$

We used matrix calculus to enable to obtain the MPC program for DFIG.

5.4 MPC laws for DFIG

The objective of this part of paper is the synthesis of a MPC in order to replace the two PI regulators of active and reactive power. These regulators were used in section 3 for DVC. Thus, we leave the classical DVC towards DVC based on MPC taking advantage of the performances and ease of implementation of MPC.

For our strategy, the outputs and inputs matrix are:

$$Y = \begin{bmatrix} P_s \\ Q_s \end{bmatrix};\ \hat{Y} = \begin{bmatrix} \hat{P}_s \\ \hat{Q}_s \end{bmatrix} and\ U = \begin{bmatrix} V^*_{rq} \\ V^*_{rd} \end{bmatrix}$$

And, the prediction of the outputs is given by:

$$\begin{bmatrix} \hat{P}_s(k+j) \\ \hat{Q}_s(k+j) \end{bmatrix} = G_j(z^{-1}) \begin{bmatrix} P_s(k) \\ Q_s(k) \end{bmatrix} + H_j(z^{-1}) \begin{bmatrix} \Delta V^*_{rq}(k+j-1) \\ \Delta V^*_{rd}(k+j-1) \end{bmatrix} + J_j(z^{-1}) \begin{bmatrix} \Delta V^*_{rq}(k-1) \\ \Delta V^*_{rd}(k-1) \end{bmatrix} \tag{29}$$

With: $G_j(z^{-1}),\ H_j(z^{-1}), and\ J_j(z^{-1})\ are\ matrix^{2\times 2}$

The next step is to find the model linking the inputs (V_{rq}, V_{rd}) to the outputs (P_s , Q_s). According to (8), the expression of reference active powers and reactive power as function of the reference rotor currents is:

$$\begin{cases} P_s^* = -\frac{3}{2}\frac{\omega_s \psi_s M}{L_s} I^*_{rq} \\ Q_s^* = -\frac{3}{2}\left(\frac{\omega_s \psi_s M}{L_s} I^*_{rd} - \frac{\omega_s \psi_s^2}{L_s}\right) \end{cases} \tag{30}$$

$\frac{\omega_s \psi_s}{L_s}$: Imposed by the Grid.

As well as, we can obtain the link between rotor voltages and rotor currents by substituting (7) and (2) into (1). Thus, the equation of the rotor voltages becomes:

$$\begin{cases} V_{rd} = R_r.I_{rd} + \left(L_r - \frac{M^2}{L_s}\right)\frac{dI_{rd}}{dt} - g.\omega_s\left(L_r - \frac{M^2}{L_s}\right) I_{rq} \\ V_{rq} = R_r.I_{rq} + \left(L_r - \frac{M^2}{L_s}\right)\frac{dI_{rq}}{dt} - g.\omega_s\left(L_r - \frac{M^2}{L_s}\right) I_{rd} + g\frac{M\omega_s\psi_s}{L_s} \end{cases} \tag{31}$$

We assume; $\sigma = \left(L_r - \frac{M^2}{L_s}\right)$: Coupling term between the two axes. It will be compensated by a delicate synthesis of the regulators in the control loop, and $\frac{M\omega_s\psi_s}{L_s}$: represents an electromotive force. The scheme of multivariable predictive control is presented by Fig. 10.

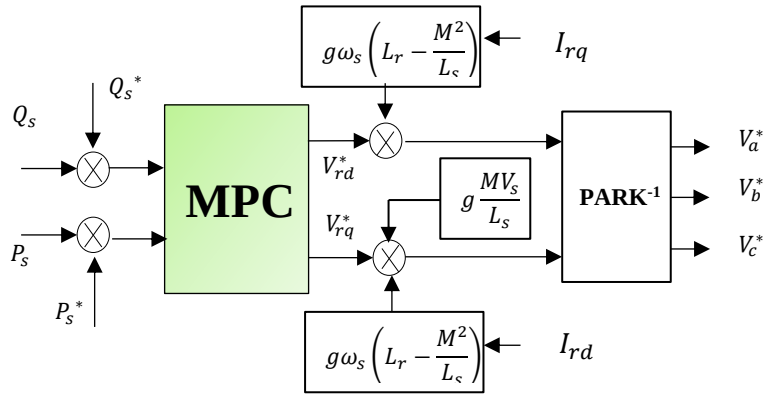

Fig. 10 scheme of MPC

On other hand, by applying the Laplace transformation to reference rotor voltages and substituting into (30), the equations linking (P_s^*, Q_s^*) to (V_{rq}^*, V_{rd}^*) are given:

$$\begin{cases} P_s^* = -\left(\frac{3}{2}\frac{V_s.M}{L_s}\right).\left(\frac{1}{R_r+\sigma.s}\right).V_{rq}^* \\ Q_s^* = -\left(\frac{3}{2}\frac{V_s.M}{L_s}\right).\left(\frac{1}{R_r+\sigma.s}\right).V_{rd}^* \end{cases} \quad (31)$$

The matrix form, (31) is written as:

$$\begin{bmatrix} P_s^* \\ Q_s^* \end{bmatrix} = -\frac{3}{2}.\begin{bmatrix} G_{11}(s) & G_{12}(s) \\ G_{21}(s) & G_{22}(s) \end{bmatrix}\begin{bmatrix} V_{rq}^* \\ V_{rd}^* \end{bmatrix} \quad (32)$$

Where:

$$G(s) = -\frac{3}{2}.\begin{bmatrix} G_{11}(s) & G_{12}(s) \\ G_{21}(s) & G_{22}(s) \end{bmatrix}, \quad (33)$$

$$with: \begin{cases} G_{11} = \frac{V_s.M}{L_sR_r+L_s\sigma.s} \\ G_{12} = 0 \\ G_{21} = 0 \\ G_{22} = \frac{V_s.M}{L_sR_r+L_s\sigma.s} \end{cases}$$

The Z-transformation of $G(s)$ for a sampling step T_e = 0.001s gives:

$$G(z^{-1}) = \begin{bmatrix} G_{11}(z^{-1}) & 0 \\ 0 & G_{22}(z^{-1}) \end{bmatrix} = z^{-1}\begin{bmatrix} \frac{-1912}{1+0.9318\,z^{-1}} & 0 \\ 0 & \frac{-1912}{1+0.9318\,z^{-1}} \end{bmatrix} \quad (34)$$

The CARIMA model is given by:

$$\begin{cases} A(z^{-1}) = \begin{bmatrix} 1+0.9318\,z^{-1} & 0 \\ 0 & 1+0.9318\,z^{-1} \end{bmatrix} \\ B(z^{-1}) = \begin{bmatrix} -1912(1+0.9318\,z^{-1}) & 0 \\ 0 & -1912(1+0.9318\,z^{-1}) \end{bmatrix} \\ C(z^{-1}) = \begin{bmatrix} 1 & 0 \\ 0 & 1 \end{bmatrix} \end{cases} \quad (35)$$

The equation (29) for j=1 is:

$$\begin{bmatrix} \hat{P}_s(k+j) \\ \hat{Q}_s(k+j) \end{bmatrix} = \begin{bmatrix} 1.9318+1.8636\,z^{-1} & 0 \\ 0 & 1.9318+1.8636\,z^{-1} \end{bmatrix}\begin{bmatrix} P_s(k) \\ Q_s(k) \end{bmatrix} + \begin{bmatrix} -1913-1781.6\,z^{-1} & 0 \\ 0 & -1913-1781.6\,z^{-1} \end{bmatrix}\begin{bmatrix} \Delta V_{rq}^*(k) \\ \Delta V_{rd}^*(k) \end{bmatrix} + \begin{bmatrix} 1847.3 & 0 \\ 0 & 1847.3 \end{bmatrix}\begin{bmatrix} \Delta V_{rd}^*(k-1) \\ \Delta V_{rd}^*(k-1) \end{bmatrix} \quad (36)$$

Where:

$$\begin{cases} G_1(z^{-1}) = \begin{bmatrix} 1.9318+1.8636\,z^{-1} & 0 \\ 0 & 1.9318+1.8636\,z^{-1} \end{bmatrix} \\ H_1(z^{-1}) = \begin{bmatrix} -1913-1781.6\,z^{-1} & 0 \\ 0 & -1913-1781.6\,z^{-1} \end{bmatrix} \\ J_1(z^{-1}) = \begin{bmatrix} 1847.3 & 0 \\ 0 & 1847.3 \end{bmatrix} \end{cases} \quad (37)$$

The function of multidimensional cost function is given as:

$$J_{GPC} = U^T(H^TH+\lambda I)U + 2U^TH^T(E-W) + (E-W)^T(E-W) \quad (38)$$

From (28), the analytic minimization gives:

$$\tilde{U} = \left(H^TH+\lambda I_{N_u}\right)^{-1}H^T(W-E) \quad (39)$$

With:

$$U = \begin{bmatrix} \begin{pmatrix} \Delta V_{rq}^*(k) \\ \Delta V_{rd}^*(k) \end{pmatrix} \\ \vdots \\ \begin{pmatrix} \Delta V_{rq}^*(k+j-1) \\ \Delta V_{rd}^*(k+j-1) \end{pmatrix} \end{bmatrix}; W = \begin{bmatrix} \begin{pmatrix} P_s^*(k+1) \\ Q_s^*(k+1) \end{pmatrix} \\ \vdots \\ \begin{pmatrix} P_s^*(k+j) \\ Q_s^*(k+j) \end{pmatrix} \end{bmatrix}$$

$$H(z^{-1}) = \begin{bmatrix} H_1(z^{-1}) & 0 & 0 \\ \vdots & H_1(z^{-1}) & 0 \\ H_j(z^{-1}) & \cdots & H_1(z^{-1}) \end{bmatrix};$$

$$E = G(z^{-1})\begin{bmatrix} P_s(k) \\ Q_s(k) \end{bmatrix} + J(z^{-1})\begin{bmatrix} \Delta V_{rd}^*(k-1) \\ \Delta V_{rd}^*(k-1) \end{bmatrix};$$

$$G(z^{-1}) = \begin{bmatrix} G_1(z^{-1}) \\ \vdots \\ G_j(z^{-1}) \end{bmatrix}; J(z^{-1}) = \begin{bmatrix} J_1(z^{-1}) \\ \vdots \\ J_j(z^{-1}) \end{bmatrix};$$

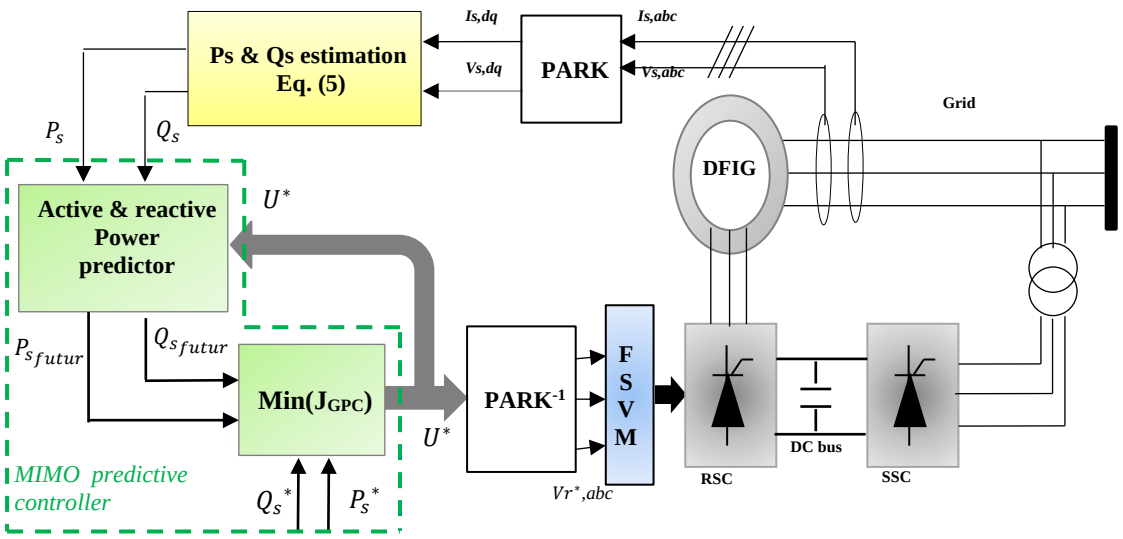

Fig. 11 control strategy diagram of DFIG

Fig. 11 shows the scheme of the DFIG control strategy. These calculations require a very powerful computer and an adequate step size.

6 Simulation results

To simulate the diagram of the fig. 11, we used the Matlab/Simulink software. The DFIG parameters are given in the following table. In the first time, we adjust the MPC parameters as N1=1, N2=5 and Nu=3. Then, we change them to N1=1, N2=10 and Nu=3 in order to improve the response time of the system. To obtain good energy performances, it needs to keep the reactive power at zero and consequently, the power factor is unity. But to test the reference tracking, we increased the reactive power reference after one second.

Table 2 DFIG parameters

Pn=*1.5 (MW)*
Vs=*398 (V)*
fs=*50 (Hz)*
P=2
Rr=*0.021* (Ω)
Rs=*0.012* (Ω)
Lr=*0.0136* (H)
Ls=*0.0137* (H)
M=*0.0135* (H)
f=*0.0024 (Nm/s)*
J=*1000 (Kg.m^2)*

Note that there is no well-specified rule for adjusting the MPC parameters, as well as for defining the logic rules. This is the only difficulty we encountered in this work. All settings are based on experiences and simulation repetitions.

6.1 Reference tracking test

The simulation results of reference tracking of stator currents, torque and active and reactive power are shown in Figs. 12-15. As shown in Figs 12, for MPC parameters N1=1, N2=5 and Nu=3, the active power and reactive power track references with a very acceptable response time which is approximately 0.03s. In the Fig. 13, the MPC parameters N1=1, N2=10 and Nu=3 give perfect results with a response time around 0.003s. On the other hand, it is clearly observed that the active power ripples, reactive power ripples and torque ripples are zero. This is undoubtedly thanks to the inverter Fuzzy SVM. The Figs. 14-15 show that the stator currents and torque track the reference without any overshoot.

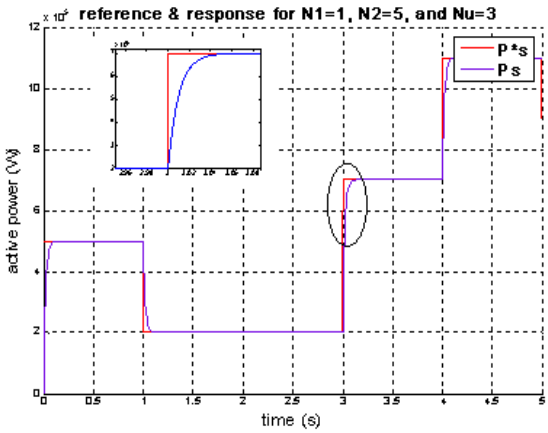

Fig. 12.a Active power for N1=1, N2=5 and Nu=3 (Reference tracking test)

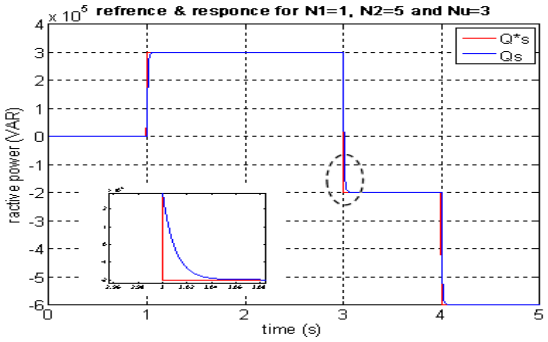

Fig. 12.b Reactive power for N1=1, N2=5 and Nu=3 (Reference tracking test)

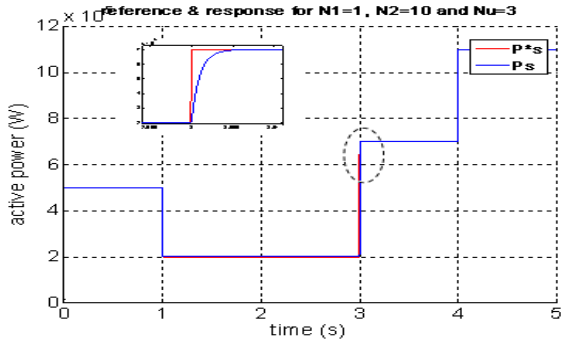

Fig. 13.a Active power for N1=1, N2=10 and Nu=3 (Reference tracking test)

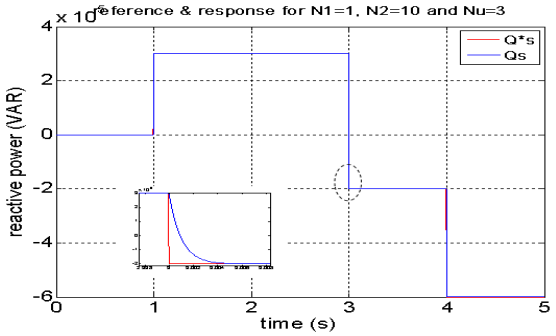

Fig. 13.b Reactive power for N1=1, N2=10 and Nu=3 (Reference tracking test)

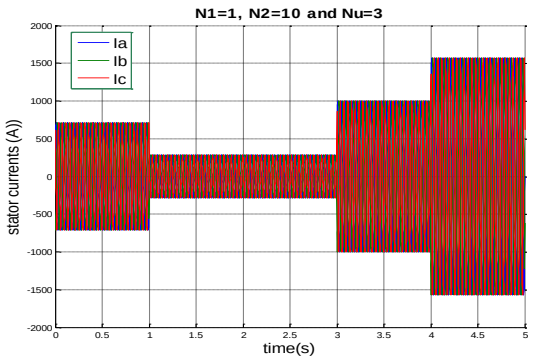

Fig. 14.a Stator currents (Reference tracking test)

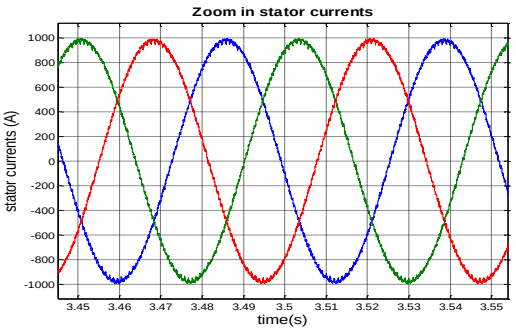

Fig. 14.b Zoom of stator currents (Reference tracking test)

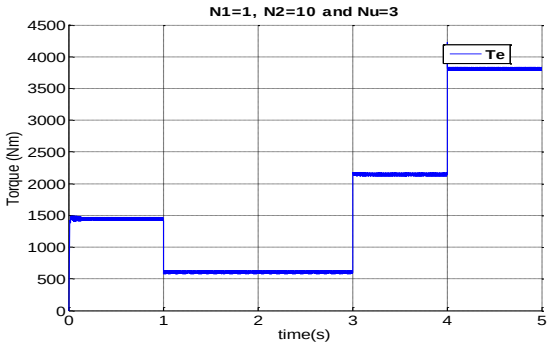

Fig. 15 Torque (Reference tracking test)

6.2 Robustness test

The robustness test consists of modifying the electrical and magnetic parameters of the machine for the purpose of testing the accuracy and the reliability of the proposed control method. In this part, the rotor and stator resistances are increased, and the rotor, stator and mutual inductances are reduced by 75% of their nominal values at the 2nd second. As a result, we can note that the MPC method is insensitive to variations of machine parameters. As shown in Figs. 16-18, active power, reactive power, torque and stator currents are not affected by these variations despite the presence of some ripples which clearly appeared after 2s of simulation.

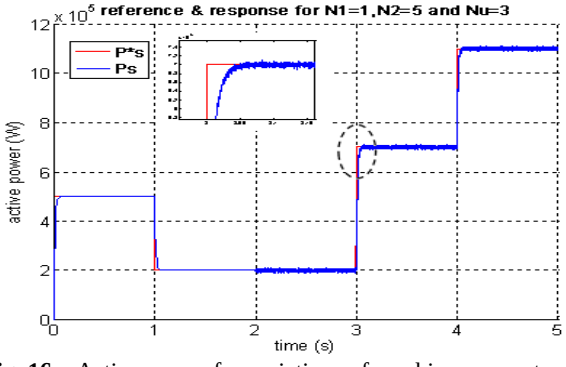

Fig. 16.a Active power for variations of machine parameters at 2s

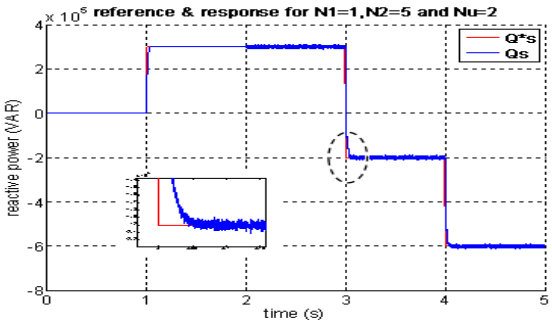

Fig. 16.b Reactive power for variations of machine parameters at 2s

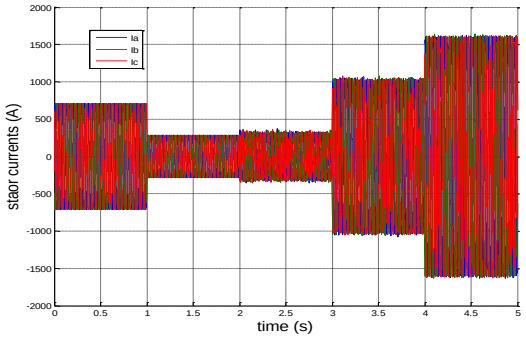

Fig. 17.a Stator currents for variations of machine parameters at 2s

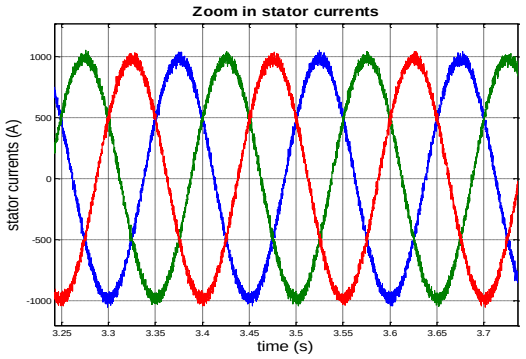

Fig. 17.b Zoom stator currents for variations of machine parameters at 2s

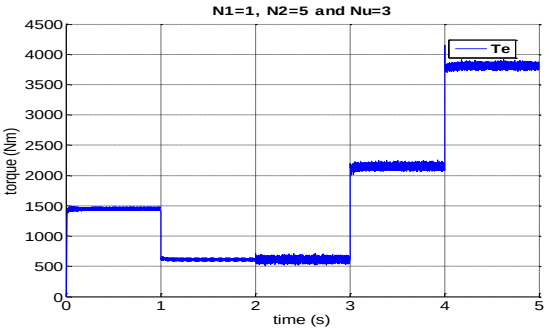

Fig. 18 Torque for variations of machine parameters at 2s

These oscillations are expected to occur, because the MPC is a model-based control. Discrepancy between the model and the real system can lead to slightly oscillatory behavior, especially during robustness testing. Nolinearity in system also produces oscillatory behavior. A short Nu (control horizon) can sometimes lead to aggressive control actions, causing chatter. These ripples can affect the grid and cause poor voltage regulation, synchronization problems in equipment relying on line frequency, increased losses, overheating in transformers and motors and malfunction of sensitive equipment. May also lead to fluctuations in the power factor, reduced efficiency in power transmission and distribution..etc.

To resolve these issues, there are several solutions. The simplest is add a derivative action to dampen oscillations. Or Using Adaptive MPC for Real-Time Adjustment. Other solution, we can use a state observatory. In our case, we generally modify the MPC parameters (the prediction and control horizons: N2 and Nu) to adapt to new DFIG parameters.

In table 3, we give a comparison of performance of the results obtained for MPC Settings.

Table 3 Performance comparison of the results obtained

MPC parametres	**N1=1, N2=5 and Nu=3**	**N1=1, N2=10 and Nu=3**
Reference tracking	perfect	perfect
Response time	acceptable	perfect
Ripples	none	none
Overtaking	Little in torqueT_e	none

7 Conclusion

In conclusion, the MPC is used for nonlinear systems with multiple inputs and multiple outputs. In this research, the MPC is employed to control the active and reactive power of a DFIG based on Fuzzy SVM technique. The proposed method is easy to implement taking into account the estimation of different variables such as the electromagnetic torque, stator active and reactive powers and stator currents. In addition, the Fuzzy SVM converter makes it possible to reduce as much as possible the ripples of the stator currents of the machine. Moreover, the combination of MPC strategy and the Fuzzy SVM-based converter enhances the performances of the machine drive compared to other classical control methods used with SVM or PWM inverter. And of course, that allows us to compensate multiple controllers with a single multivariable controller. As a result, we obtain a reduced control system size with less computations.

This work can be developed to integrate with machine learning and optimization techniques to significantly improve the performance, efficiency and reliability of DFIG systems. And can contribute to the advancement of renewable energy technologies.

References

[1] L.Saihi, B. Berbaoui and H. Glaoui,"Robust Control H∞ Fuzzy of a Doubly Fed Induction Generator Integrated to Wind Power System," *Majlesi Journal Of Electrical Engineering*, Vol. 14, No. 1, pp.59-69, March 2021.

[2] H. Benbouhenni, Z. Boudjema and A. Belaidi,"Direct Vector Control of a DFIG Supplied by an Intelligent SVM Inverter for Wind Turbine System," *Iranian Journal of Electrical and Electronic Engineering*, Vol. 15, No. 1, pp.45-55, March 2019.

[3] Z. Boudjema, R. Taleb, Y. Djeriri and A.Yahdou,"A novel direct torque control using second order continuous sliding mode of a doubly fed induction generator for a wind energy conversion system," *Turkish Journal of Electrical Engineering & Computer Sciences*, Vol. 25, No. 2, pp.965-975, 2017.

[4] H. Benbouhenni, Z. Boudjema and A. Belaidi,"Indirect Vector Control of a DFIG Supplied by a Two-Level FSVM Inverter for Wind Turbine System," *Majlesi Journal of Electrical Engineering*, Vol. 13, No. 1, pp.45-54, March 2019.

[5] S.Labdai, N. Bounar, A. Boulkroune, B. Hemici and L. Nezli,"Artificial neural network-based adaptive control for a DFIG-based WECS," *ISA Transactions*, Vol.128, pp.171-180, September 2022.

[6] S. Abazari and S. Farajzadeh Dehkordi,"Sliding-Mode Control for a DFIG-Based Wind-Power Generation System with Series Grid-Side Converter under Unbalanced Grid Voltage Conditions," *Scientia Iranica*, Vol. 25, No. 3, pp.1507-1522, 2018.

[7] A. Berkani, K. Negadi, T. Allaoui, F. Marignetti "Sliding mode control of wind energy conversion system using dual star synchronous machine and three level converter," *TECNICA ITALIANA-Italian Journal of Engineering Science*, Vol. 63, No. 2-4, pp. 243-250, 2019.

[8] L. Djilali, E. Sanchez; M. Belkheiri,"Neural sliding mode field oriented control for DFIG based wind turbine," *in IEEE International Conference on Systems, man and Cybernetics (SMC)*, Banff, Canada, October 2017

[9] B. Bossoufi, M. Karim, A. Lagrioui, M. Taoussi and M L ElHafyani,"Backstepping control of DFIG generators for wide-range variable-speed wind turbines," *Int. J. Automation and Control*, Vol. 8, No. 2, pp 122-140, 2014.

[10] M. El-Azzaoui, H. Mahmoudi and K. Boudaria,"Backstepping control of wind and photovoltaic hybrid renewable energy system," *Internationale Journal of Power Electronics and Drive Systems*, Vol. 7, No. 3, pp. 677–686, 2016.

[11] H. Benbouhenni, Z. Boudjema and A. Belaidi,"Neuro-Second Order Sliding Mode Control of a DFIG Supplied by a Two-Level NSVM Inverter for Wind Turbine System," *Iranian Journal of Electrical and Electronic Engineering*, Vol. 14, No. 4, pp. 362-373, December 2018.

[12] V. Meenakshi, G. D. Anbarasi and J. S. Paramasivam,"Space vector modulation technique applied to doubly fed induction generator," *Indian Journal of Science and Technology*, Vol. 8, pp 1–8, 2015.

[13] M. Gaballah, M. El-Bardini, S. Sharaf and M. Mabrouk, "Implementation of space vector PWM for driving two level voltage source inverters," *Journal of Engineering Sciences*, Vol. 39, No. 4, pp. 871–884, 2011.

[14] A. Khati, A. Kansab, R. Taleb and H. Khouidmi,"Current predictive controller for high frequency resonant inverter in induction heating," *International Journal of Electrical and Computer Engineering*, Vol. 10, No. 1, pp. 255-264, February 2020.

[15] H. Khouidmi, A. Massoum, "Predictive Control Based Speed, Torque and Flux Prediction of a Double Stator Induction Motor" Majlesi Journal *of Electrical Engineering*. Vol. 13, No. 1, pp. 65-77, March 2019.

[16] J. Lyu, W. Hu, F. Wu, K. Yao, J. Wu, "A new DPWM Method to Suppress the Low Frequency Oscillation Of The Neutral-Point Voltage For NPC Three-Level Inverters," *Journal of Power Electronics*, Vol. 15, No.5, pp. 1207-1216, 2015.

[17] S. Massoum, A. Meroufel, A. Massoum, P. Wira, "A Direct Power Control of the Doubly-Fed Induction Generator based on the SVM Strategy," *Elektrotehniski Vestnik*, Vol. 45, No. 5, pp. 235-240, 2017

[18] M. Gaballah and M. El-Bardini,"Low cost digital signal generation for driving space vector PWM inverter;" *Ain Shams Engineering Journal*, Vol. 4, pp. 763–774, 2013.

[19]Y. Guo, H. Long, "Self Organizing Fuzzy Sliding Mode Controller for The Position Control of A Permanent Magnet Synchronous Motor Drive, " *Ain Shams Engineering Journal*, Vol. 2, pp. 109-118, 2011.

[20] H. Benbouhenni, "36 Sectors DTC based on fuzzy logic of sensorless induction motor drives," *Research & Reviews: Journal of Engineering and Technology*. Vol. 7, No. 1, pp. 24–32, 2018.

[21] A. Berkani, MH. Ghazwani, K. Negadi, L. Hadji, A. Alnujaie, HA. Ghazwani, "Predictive control and modeling of a point absorber wave energy harvesting connected to the grid using a LPMSG-based power converter," *Ocean Systems Engineering*, Vol. 14, No. 1, pp. 17-52, March 2024.

[22] R. Rezavandi, D. A. Khaburi, M. Siami, M. Khosravi, S. Heshmatian," Model Predictive Control of a BCDFIG With Active and Reactive Power Control Capability for Grid-Connected Applications *Iranian Journal of Electrical and Electronic Engineering*, Vol. 17, No. 2, pp. 1-11, June 2021.

[23] L. Bossi, C.Rottenbacher, G.Mimmi, L.Magni,"Multivariable Predictive Control for Vibrating Structures: An application," *Control Engineering Practice* Vol.19, No. 10, pp. 1087–1098, October 2011.

[24] A.Younesi, S. Tohidi, M.R. Feyzi. "Fixed switching frequency scheme for current predictive control of DFIG," *Journal of Energy Management and Technology*," Vol. 6, No. 2, pp. 73-82, 2022.

[25] H. Khouidmi, A. Massoum,"Neural Networks Generalized Predictive Speed Controller for Vector Controlled Double Stator Induction Motor," *Majlesi Journal of Mechatronic Systems*, Vol. 03, No. 2, pp. 13-18, 2014.

[26] A.F. Syed, Ch.A. Fahad, H. Desa, A T. Hussain,"Model Predictive Controller-based, Single Phase Pulse Width Modulation (PWM) Inverter for UPS Systems," *Journal of Applied Sciences, Acta Polytechnica Hungarica*, Vol. 11, No. 6, pp. 23-38, 2014.

A. khati received his M.SC degree in electrical engineering in 2014 from the Hassiba Benbouali University, Chlef, Algeria. And received his Ph.D degree in Electrical Engineering in 2020 from the same University. He is currently head of mechanical engineering department at the Chlef university. His research interest includes intelligent control strategies, electrical machine drives and robotics.